Impurity spin texture at the critical point between Néel-ordered and valence-bond-solid states in two-dimensional SU(3) quantum antiferromagnets

Argha Banerjee,[1] Kedar Damle,[1] and Fabien Alet[2]

[1]*Tata Institute of Fundamental Research, 1, Homi Bhabha Road, Mumbai 400005, India*
[2]*Laboratoire de Physique Théorique, Université de Toulouse, UPS, (IRSAMC), F-31062 Toulouse, France*

We study the impurity physics at a continuous quantum phase transition from an SU(3) symmetric Néel-ordered state to a valence-bond-solid state that breaks lattice symmetries, using quantum Monte Carlo techniques. This continuous transition is expected to be an example of "deconfined criticality" in an SU(3) symmetric system. We find that the spin-texture induced by a missing-spin defect at the transition takes on a finite-size scaling form consistent with expectations from standard scaling arguments at a scale-invariant quantum critical point, albeit with significant subleading power-law finite size corrections that we analyze in detail. Together with recently found logarithmic violations of scaling at similar continuous transitions in the SU(2) case, our results provide indirect evidence of the existence of operators that become marginal as N is reduced to 2 in the field theoretical description of these deconfined critical points.

I. INTRODUCTION

Impurity effects, arising from naturally occurring or intentionally introduced defects, have been exploited often as probes of the low-temperature physics of various condensed matter systems. The characteristic response pattern that results from the presence of impurities usually contains spatially resolved information which provides clues about the nature of the low-temperature phase, the presence of long-range order, and the role of quantum fluctuations and other competing orders that are suppressed in the bulk but may be realized close to the impurity. Such clues are crucial in the context of materials with strong electronic correlations whose physics is not as well understood as ordinary metals, and such an approach has therefore been heavily used in experiments on unconventional superconductors and Mott insulating antiferromagnets.[1]

On the theoretical front, the very nature of these strongly correlated systems makes detailed analytical solutions difficult even for simplified models. Furthermore, mean-field methods often fail to capture the strong correlations well enough to be reliable. In cases where efficient numerical computations are possible, large-scale high-precision numerical studies can be used to access the physics of such systems. Other approaches that have had some degree of success include "large-N" approximation schemes, in which the symmetry group of the physical problem [for instance, SU(2) of spin-rotation invariance] is enlarged [for instance, replacing SU(2) by SU(N)], and the resulting generalization solved by approximations that become exact in the large-N limit. This approach has been particularly useful and influential in the study of quantum magnetism, and the generalization of the SU(2) spin rotational symmetry to SU(N) has played a key role in our understanding of the magnetism of strongly correlated Mott insulators.

For instance, the analysis of the SU(N) Heisenberg model by Read and Sachdev[2,3] provided the first insights regarding the manner in which a Néel-ordered SU(2) antiferromagnet can be destabilized by quantum fluctuations in the antiferromagnetic order to form a valence-bond solid (VBS). In their analysis, Read and Sachdev considered an SU(N) generalization in which A-sublattice sites of the square lattice carry an SU(N)

representation with $m = 1$ rows and n_c columns, while B-sublattice sites carried a representation with $N - m \equiv N - 1$ rows and n_c columns. Assuming short-ranged Néel order, but making no assumptions about the presence of long-range Néel order, Read and Sachdev argued that the physics of such magnets can be described by a CP^{N-1} field theory coupled to a (compact) U(1) gauge field in two spatial dimensions, with a dimensionless coupling g that is a function of both n_c and the microscopic details of the interactions between spins (for instance, the strength of additional exchange or ring-exchange terms). This CP^{N-1} theory admits point-like space-time "hedgehog" defects which correspond to monopoles in the compact U(1) gauge field. These hedgehogs carry Berry phases that depend on their spatial locations and the value of n_c. In the antiferromagnetic phase stabilized at small g, these hedgehogs are energetically suppressed, and their Berry phases can be ignored. Conversely, the VBS phase corresponds to a "condensate" of these hedgehogs, with their position-dependent Berry phases being responsible for the spontaneous breaking of spatial translational symmetry characteristic of the VBS phase.

Senthil *et al.*[4] used this picture of the two phases to argue that the quantum phase transition between them in two-dimensional SU(2) antiferromagnets can be generically a continuous transition. This is in conflict with expectations from the usual Landau theory approach, which predicts that a direct transition between these two phases should generically be first order. In the analysis of Senthil *et al.*, this transition can be generically continuous *if* quadrupled hedgehog defects,[5] which are known to be irrelevant in a renormalization group sense in the large-N limit, remain irrelevant in the $N = 2$ case. As a result of the irrelevance of hedgehog defects, the "natural" description of this transition is then in terms of "deconfined" spinon fields of a *noncompact* CP^1 model (NCCP^1) coupled to a noncompact U(1) gauge field, rather than the antiferromagnetic vector order parameter field corresponding to Néel ordering on one side of the transition or the complex order parameter corresponding to VBS order on the other.

This prediction of a deconfined critical point separating the Néel and VBS phases motivated several numerical studies that tried to test its validity in two quite different ways. One of these

involved the numerical study of specific lattice discretizations of the NCCP[1] field theory itself. Using such an approach, Kuklov *et al.* studied a lattice discretization of the NCCP[1] field theory and found that it admits a weakly first-order transition[6] with finite correlation length, rather than a critical point with diverging correlation length. On the other hand, Motrunich and Vishwanath studied a different lattice discretization[7] and found that it admits a critical point whose properties are expected to provide a good description of the generically continuous Néel-VBS transition. However, this has in turn been contested in subsequent work.[8]

The second set of studies focused instead on microscopic spin models capable of displaying such Néel-VBS transitions. The most studied of these are the *J*-*Q* models constructed by Sandvik,[9] in which a direct transition from Néel to VBS order is driven by the competition between four-spin plaquette interactions (*Q* terms) that favor VBS order on the square lattice and two-spin exchange interactions (*J* terms) that favor two-sublattice Néel order on the square lattice. While initial studies of the *J*-*Q* models[9–12] did not fully resolve the nature of this transition, more recent work[13] has convincingly demonstrated the generically continuous nature of the Néel-VBS transition in this class of SU(2) symmetric $S = 1/2$ models on the square lattice.

This most recent study of the bulk Néel-VBS transition[13] as well as recent work on impurity effects at this transition[14] both lead to another remarkable conclusion: although the Néel-VBS transition in SU(2) symmetric $S = 1/2$ systems on the square lattice is indeed continuous, logarithmic violations of scaling behavior, of the type that can arise when the critical theory contains marginally irrelevant operators, are also present at the critical point. These logarithmic effects could be the cause of the conflicting conclusions from the earlier numerical studies of this transition in the *J*-*Q* models, with some studies[9,10,12] interpreting their results in terms of a continuous transition with conventional scaling properties, and other studies interpreting very similar data in terms of a weakly first-order transition.[11]

It is therefore natural to ask if this reflects the fact that quadrupled monopole operators, which are known to be strongly irrelevant in the large-*N* limit,[4] actually become marginally irrelevant in the physical $N = 2$ theory. While this question cannot be directly addressed by computational studies in the absence of fresh insights on the field theory side, it does provide a strong motivation to study similar Néel-VBS transitions on the square lattice in microscopic SU(*N*) spin models with enlarged symmetry ($N > 2$). If these transitions are continuous, it is of great interest to see whether they obey predictions from standard scaling theory without logarithmic violations. This is the question we address in this work.

To do this, we focus on the SU(3) *J*-*Q* model[12] which has antiferromagnetic exchange interactions *J* between nearest neighbors and a four-spin coupling *Q* between sites belonging to a plaquette. In the language of Read and Sachdev,[3] the spins in this model carry a representation with $n_c = 1$ columns and $m = 1$ rows on the *A* sublattice and $n_c = 1$ columns and $N - m \equiv N - 1$ rows on the *B* sublattice, with $N = 3$ in the case of SU(3). This model generalizes the SU(*N*) antiferromagnetic model with purely nearest-neighbor exchange that was studied in earlier works,[15,16] which found that the ground state is Néel

ordered for $N = 3$ and $N = 4$. From the work of Lou *et al.*[12] and Kaul,[17] it is known that this SU(3) model has a continuous transition between this Néel-ordered state and a VBS-ordered singlet ground state as *Q* is increased beyond $Q_c/J \approx 0.502$.

Here, we study the zero-temperature impurity spin texture that is induced by a single vacancy in the lattice at this SU(3) transition point, and confront our computed results with predictions from finite-size scaling theory[14,18,19] that rely on the scale invariance of the underlying quantum critical point. By a careful analysis of the scaling properties of the Fourier components of the spin texture near wave vectors $\mathbf{k} = \mathbf{0}$ and $\mathbf{k} = \mathbf{Q}$ [where $\mathbf{Q} \equiv (\pi, \pi)$ is the antiferromagnetic ordering wave vector on the square lattice], we conclude that the Néel-VBS transition in such SU(3) magnets on the square lattice obeys finite-size scaling forms expected at a scale-invariant quantum critical point, albeit with noticeable subleading finite-size corrections to scaling. In other words, the hitherto unidentified marginal operator in the $N = 2$ critical theory is no longer marginal in the $N = 3$ case. The recent work of Kaul[17] addresses similar issues, albeit considering *bulk* properties of the transition in the SU(3) and SU(4) *J*-*Q* models.

The plan of the paper is as follows. We briefly introduce the SU(*N*) *J*-*Q* model in Sec. II. We then describe the projector quantum Monte Carlo method used to simulate the SU(*N*) *J*-*Q* model with a single nonmagnetic impurity in Sec. III, first describing our choice of basis in Sec. III A, and then outlining how existing algorithms must be modified to account for both the existence of the SU(*N*) symmetry and of a spinless impurity. We then present and analyze our numerical results for the impurity-induced spin texture at the critical point of the SU(3) *J*-*Q* model in Sec. IV. Finally, we discuss implications of our results and present our conclusions in Sec. V.

II. MODEL

We consider a system made of N_A *A*-sublattice sites with "spins" that carry the defining representation **N** of SU(*N*) and N_B *B*-sublattice sites at which spins carry the conjugate representation **N***. Following Refs. 12,15,16, we write the Hamiltonian as

$$H = -J \sum_{\langle ij \rangle} P_{ij} - Q \sum_{\langle ij \rangle \langle kl \rangle} P_{ij} P_{kl}, \qquad (1)$$

where $P_{ij} = -\frac{1}{N} \mathcal{A}_\beta^\alpha(i) \mathcal{A}_\alpha^\beta(j)$, $\mathcal{A}_\beta^\alpha$, the generators of the SU(*N*) algebra satisfy the relations $[\mathcal{A}_\beta^\alpha(i), \mathcal{A}_\nu^\mu(j)] = \delta_{ij}(\delta_{\alpha\nu} \mathcal{A}_\beta^\mu(i) - \delta_{\mu\beta} \mathcal{A}_\nu^\alpha(i))$. The *J* term acts on links $\langle ij \rangle$ connecting nearest-neighbor pairs of sites of the square lattice, while the *Q* term acts on a pair of parallel nearest-neighbor links $\langle ij \rangle \langle kl \rangle$ on the same plaquette of the square lattice. As indicated above, we choose to represent these generators in two different representations on the two sublattices of the square lattice. On the *A* sublattice, we use the $N \times N$ matrices of the fundamental representation **N** acting on states $|\alpha\rangle$ ($\alpha = 1, 2, \ldots, N$) that live on each *A*-sublattice site, while on the *B* sublattice, the SU(*N*) generators are represented in terms of matrices of the complex conjugate **N*** of the fundamental representation that act on the basis states $|\bar{\alpha}\rangle$ on each *B*-sublattice site.

The physics of this antiferromagnetic SU(*N*) model becomes clear upon noting that when *i* and *j* belong to different

sublattices, P_{ij} is actually a projector onto the SU(N) singlet **1** contained in the decomposition of $\mathbf{N} \otimes \mathbf{N}^*$. By analogy to the SU(2) case, the J term is thus expected to favor long-range antiferromagnetic order in the SU(N) spins, while the Q term favors a valence-bond solid in which a particular pattern of pairs of spins lock into SU(N) singlets, breaking the symmetry of lattice translations.

As is well-known, this antiferromagnetic SU(N) model can also be thought of in terms of SU(2) spin $S = (N - 1)/2$ variables interacting via a Hamiltonian with enhanced SU($2S + 1$) symmetry. More precisely, we make the correspondence $|\alpha\rangle \equiv |S^z = \alpha - S - 1\rangle$ for $\alpha = 1, 2, \ldots, N$ on the A sublattice, and $(-1)^{\alpha - N}|\bar{\alpha}\rangle \equiv |S^z = S + 1 - \alpha\rangle$ for $\alpha = 1, 2, \ldots, N$ on the B sublattice. In this language, the SU(N) singlet state between an A-sublattice spin and a B-sublattice spin $|\phi_{ij}\rangle = \frac{1}{\sqrt{N}} \sum_{\alpha=1}^{N} |\alpha\rangle_i \otimes |\bar{\alpha}\rangle_j$ can be rewritten as $|\phi_{ij}\rangle = \frac{1}{\sqrt{2S+1}} \sum_{m=-S}^{S} (-1)^{m-S} |S_i^z = m\rangle \otimes |S_j^z = -m\rangle$ and thus, the matrix elements of P_{ij} are explicitly given by

$$\langle m_i', m_j' | P_{ij} | m_i, m_j \rangle = \frac{(-1)^{m_i + m_i' - 2S}}{2S + 1} \, \delta_{m_i, -m_j} \, \delta_{m_i', -m_j'}. \quad (2)$$

III. METHOD

A. Choice of basis

Our goal is to compute expectation values of local operators in the ground-state of Hamiltonian (1) for a system with a given (odd or even) number of sites. For the SU(2) invariant, nearest-neighbor $S = 1/2$ antiferromagnet at $Q = 0$ on a finite bipartite lattice, we know from the Lieb-Mattis theorem[20] that the ground state is a $S_{\text{tot}} = 0$ singlet when the total number of sites is even, and is doubly degenerate corresponding to $S_{\text{tot}} = 1/2$ when the number of spins is odd. Unfortunately, it does not appear possible to come up with a simple extension of the Lieb-Mattis argument that would lead to such a result for Hamiltonian (1) when $N > 2$, even in the case with $Q = 0$. The main obstruction is that the Perron-Frobenius theorem (at the heart of the original Lieb-Mattis proof) cannot be used for the Hamiltonian in the total S^z basis since this Hamiltonian is known to be *reducible* in each S^z sector.[21]

Even though we have been unable to prove the corresponding statement, we nevertheless expect that the ground state of Eq. (1) belongs to the SU(3) singlet sector when the number of sites is even. When the number of A sublattice sites N_A equals $N_B + 1$, where N_B is the number of B sublattice sites, we similarly expect, by analogy with the Lieb-Mattis result for $S = 1/2$ SU(2) antiferromagnets, that the ground state of this antiferromagnetic Hamiltonian lies in the sector corresponding to the smallest irreducible representation of SU(N) contained in the decomposition of a tensor product of $N_B + 1$ copies of **N** and N_B copies of **N***. Since the smallest dimensionality irreducible representation in this decomposition is **N**, this then suggests that the ground-state multiplet of an SU(N) antiferromagnet with one extra A-sublattice site will carry representation **N**. In the language of the equivalent $S = 1$ system for $N = 3$, this translates to the statement that the ground state for a system with $N_A = N_B + 1$ has total spin $S_{\text{tot}} = 1$.

We have checked both these expectations for the pure Heisenberg model in one dimension with density matrix renormalisation group calculations for L up to 64, and with the Green's function Monte Carlo method for the model Eq. (1) with $L = 4$ (for some values of J/Q). In all cases studied, the ground state was found to be in the expected sector. We further found (for the samples studied) that the lowest-energy levels in all spin sectors of the equivalent spin $S = (N - 1)/2$ Hamiltonian follow (a weaker version of) the Lieb-Mattis ordering:[20] $E_0(S + 1) \geqslant E_0(S)$.

For systems with an even number of sites, the SU(N) singlet sector is spanned by SU(N) valence bonds, where each A-sublattice spin forms an SU(N) singlet with a B-sublattice spin,[16] and the efficient projection algorithm of Sandvik and Evertz can be readily generalized[12,16] to project out the ground state written in this basis and sample expectation values of various operators. When the number of A sublattice sites is larger than the number of B sublattice sites by 1, and the ground state is N-fold degenerate (and carries the fundamental representation **N**), we can proceed in a manner entirely analogous to the approach followed in Ref. 22. There, the SU(2) singlet sector algorithm of Sandvik and Evertz was generalized to cases where the ground state of an SU(2) symmetric $S = 1/2$ antiferromagnet has total spin $S_{\text{tot}} = 1/2$ due to the presence of one extra A-sublattice site.

To do this, we use a modified basis that leaves one A-sublattice site a_f "free" (in an arbitrary state $|\alpha\rangle_{a_f}$), and allows the remaining $N_A - 1$ A-sublattice spins to form SU(N) singlets with the $N_B = N_A - 1$ B-sublattice spins. The full basis is thus obtained by allowing all choices of free site a_f, all choices of state $|\alpha\rangle_{a_f}$ for this free site, and all valence-bond pairings possible between the other $N_A - 1$ A-sublattice spins and the N_B B-sublattice spins. Using an argument completely analogous to those given in Ref. 22 for the SU(2) case, it is easy to see that this basis spans the ground-state sector of this SU(N) magnet with $N_B = N_A - 1$ B-sublattice sites and N_A A-sublattice sites, because states from this basis can be used to construct *all* states of the SU(N) valence-bond basis of Beach *et al.*[16] and Lou *et al.*[12] for the singlet sector of the auxiliary system obtained by adding to the odd-site system one extra B-sublattice spin that carries the representation **N***.

B. Modified algorithm and estimators

The SU(N) generalization[12,16] of the Sandvik-Evertz algorithm[23] can be modified to account for an odd number of sites and an N-fold degenerate ground state in a very simple way, following Ref. 22. In this approach, the ground state is obtained by stochastically sampling the action of $(-H)^m$ (with some large power $m \sim L^3$ for an $L \times L$ system of linear size L) on an initial trial state $|\psi_S\rangle$ in the ground-state sector with $S_{\text{tot}} = S_{\text{tot}}^z = S$ with $S = (N - 1)/2$ (in the equivalent spin representation). More specifically, the "space-time loop" representation[23] of $\langle \psi_S | (-H)^{2m} | \psi_S \rangle$ has, apart from the closed space-time loops that can take on any one of the $2S + 1$ states,[12,23] exactly one extra "open string" (as in Ref. 22) with alternating A-sublattice and B-sublattice nodes which are fixed to be in the $S^z = +S$ and $S^z = -S$ state, respectively. Unlike the closed loops, the open string thus has only one allowed state. We use loop updates to flip between the $2S + 1$

allowed states of each closed loop, exactly as in the SU(N) algorithm of Ref. 12, but do not change the state of the open string. All other aspects of the algorithm remain essentially unchanged, apart from the fact that valence-bond updates are designed in our case to allow the free site a_f to move around with weights derived from the trial state $|\psi_S\rangle$ written in our chosen basis. To obtain a convenient representation of the overlap between $(-H)^m|\psi_S\rangle$ and $\langle\psi_S|(-H)^m$, we follow Sandvik and Evertz and keep track of space-time loops that cross the central space-time "slice" to obtain the valence-bond loop representation of this overlap. However, as in Ref. 22, we also need to keep track of the open string, since it necessarily crosses the central space-time slice, and therefore gives rise to an open string in the valence-bond loop representation of this overlap.

Generalizing the computations of Ref. 22 to the SU(N) case, one can obtain modified estimators for various physical quantities in terms of this valence-bond loop representation of the overlap between $(-H)^m|\psi_S\rangle$ and $\langle\psi_S|(-H)^m$. As we focus here on the impurity-induced spin texture, we are interested mainly in the computation of the expectation value $\langle S^z(\mathbf{r})\rangle$ in the ground state with a total z component of spin $S^z_{\text{tot}} = S$. It is quite easy to see that this takes on a very simple expression in terms of the probability, $P_{\text{open}}(\mathbf{r})$, that the open string passes through the site $\mathbf{r}$:

$$\langle S^z(\mathbf{r})\rangle = (-1)^{\mathbf{r}} S P_{\text{open}}(\mathbf{r}).$$

This is because the contributions of all closed loops in the valence-bond overlap cancel out since a site covered by a closed loop is equally likely to be in any S^z state.

Below, we use this to study the impurity-induced spin texture created by a missing-site defect at the critical point of the SU(3) J-Q model Eq. (1).

IV. SPIN TEXTURE AT CRITICAL POINT

A. Definition and measurements of the spin texture

The impurity spin-texture $\langle S^z(\mathbf{r})\rangle$ in the ground state with $S^z_{\text{tot}} = S$ has an alternating part $\Phi^n(\mathbf{r})$ that oscillates in sign between the two sublattices of the square lattice, and a uniform part $\Phi^u(\mathbf{r})$ that varies slowly in space. It is therefore useful to consider the Fourier transform

$$S^z(\mathbf{k}) = \sum_{\mathbf{r}} \langle S^z(\mathbf{r})\rangle \exp(i\mathbf{k}\cdot\mathbf{r}),$$

defined for wave vectors $\mathbf{k} = 2\pi\mathbf{m}/L$ [where $\mathbf{m} \equiv (m_x, m_y)$, with $m_{x/y} = 0, 1, \ldots, L-1$]. This two-component description of the real-space texture implies that $S^z(\mathbf{k})$ is expected to have two peaks, one at $\mathbf{k} = 0$ of magnitude S (reflecting the fact that $S^z_{\text{tot}} = +S$ in the ground state under consideration), and the other at $\mathbf{k} = \mathbf{Q} \equiv (\pi, \pi)$, reflecting the tendency to Néel order.

If the underlying quantum critical point is scale invariant, one expects that both the uniform and the alternating parts of the real-space spin texture obey the predictions of standard finite-size scaling theory which assumes that the system size

L is the only length scale left in the problem at criticality. One therefore expects[18,19]

$$\Phi^u(\mathbf{r}) = \frac{1}{L^2} f^u(\mathbf{r}/L),$$

$$\Phi^n(\mathbf{r}) = \frac{1}{L^{(1+\eta/2)}} f^n(\mathbf{r}/L),$$

where η is the bulk anomalous exponent associated with the Néel-order parameter, f^u and f^n are the scaling forms for the uniform and alternating signals, and this scaling form is expected to work at all $|\mathbf{r}| \gg 1$. Since it is difficult to unambiguously identify the alternating and uniform parts of the texture in real space, we find it convenient to go to Fourier space and note that these scaling expectations imply that $S^z(\mathbf{k})$ obeys corresponding scaling laws in the vicinity of these two peaks:

$$S^z(\mathbf{q}) = g_0(\mathbf{m}) \quad \text{for } |\mathbf{q}| \ll \pi/2,$$
$$S^z(\mathbf{Q}+\mathbf{q}) = L^{(3-\eta)/2} g_{\mathbf{Q}}(\mathbf{m}) \quad \text{for } |\mathbf{q}| \ll \pi/2, \tag{3}$$

where $\mathbf{m} \equiv \mathbf{q}L/2\pi$.

Our strategy is thus straightforward. We use the projector quantum Monte Carlo technique to obtain high-precision data on the impurity spin texture induced by a single vacancy in $L \times L$ samples with L even and periodic boundary conditions. We use the latest estimate[17] of the transition point $J/Q|_c \sim 1.9908$ (we have checked that our analysis holds for other slightly different estimates of $J/Q|_c$). We analyze the corresponding Fourier transform $S^z(\mathbf{k})$ near the peaks at $\mathbf{k} = 0$ and $\mathbf{k} = \mathbf{Q}$ and ask if the scaling expectations outlined above are met.

We begin our analysis with the peak at zero wave vector, since this part of the analysis does not even need knowledge of the bulk anomalous exponent η. We focus on $|S^z(\mathbf{q})|$ and consider its dependence on $\mathbf{m} = \mathbf{q}L/2\pi$ for various L ranging from $L = 48$ to $L = 128$. The hypothesis of scale invariance requires that all these data should define a single universal function of $\mathbf{m}$. In other words, at fixed $\mathbf{m}$, data from various system sizes L should fall on top of each other. Our results are shown in the left panel of Fig. 1 which plots $|S^z(\mathbf{q})|$ as a function of $|\mathbf{m}|$ (the data are averaged over all available $\mathbf{m}$ that correspond to a given $|\mathbf{m}|$).

We see that the numerical data do seem to scale reasonably well. However, when we zoom in (inset to Fig. 1), small deviations from perfect scaling are visible. Next we investigate the behavior near wave vector $\mathbf{Q}$, using the best-fit value $\eta = 0.18$ obtained by fitting $|S^z(\mathbf{Q})|$,[24] and ask if $|S^z(\mathbf{Q} + 2\pi\mathbf{m}/L)|$ collapses onto a single curve when all the data for various sizes L are plotted against $\mathbf{m}$. This is shown in the right panel of Fig. 1. Again, we see that the data do scale reasonably well, but deviations from perfect scaling are visible upon zooming in (inset to Fig. 1). For both peaks, we also note that the deviations from scaling are noticeably smaller than in the corresponding peaks for the SU(2) case (see Fig. 1 of Ref. 14). However, a detailed analysis of these small deviations from scaling is needed to explore this in more quantitative terms.
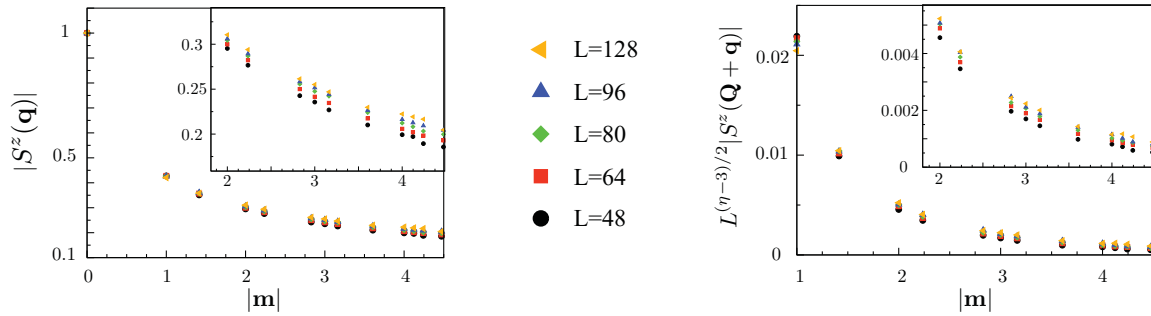
FIG. 1. (Color online) $\mathbf{m} = \mathbf{q}L/2\pi$ dependence of $|S^z(\mathbf{k})|$ at the Néel-VBS transition in the SU(3) symmetric J-Q model, for $\mathbf{k} = \mathbf{Q} + \mathbf{q}$ (right panel) and $\mathbf{k} = \mathbf{q}$ (left panel). The value of the bulk exponent $\eta = 0.18$ used here is obtained from a fit of the L dependence of $|S^z(\mathbf{Q})|^{24}$. Insets zoom in on the small deviations from perfect scaling.

B. Finite-size effects in the spin texture

It is important to understand these deviations from scaling and to ask if they can be understood in terms of subleading finite-size corrections to scaling of the standard form expected at a scale-invariant quantum critical point. To do this, we note that scaling theory would predict that the dimensionless argument $\mathbf{m}$ should acquire subleading corrections that transform it to $[1 + \delta_0(\mathbf{m})(l_0/L)^{p_0}]\mathbf{m}$, where the power $p_0 > 0$ is a property of the renormalization group flows toward the fixed point describing this scale-invariant critical point, $\delta_0(\mathbf{m})$ is a function of the dimensionless variable $\mathbf{m}$, and l_0 is a microscopic length scale that depends on the details of the Hamiltonian under study. A similar ansatz would be expected to hold for the peak centered at the antiferromagnetic wave vector, with δ_0 replaced by $\delta_\mathbf{Q}$, l_0 by $l_\mathbf{Q}$, and p_0 by $p_\mathbf{Q}$. In other words, we modify Eq. (3) to now read

$$S^z(\mathbf{q}) = g_0\big(\mathbf{m} \cdot \big[1 + l_0^{p_0}\delta_0(\mathbf{m})/L^{p_0}\big]\big),$$
$$S^z(\mathbf{Q} + \mathbf{q}) = L^{\frac{3-\eta}{2}} g_\mathbf{Q}\big(\mathbf{m} \cdot \big[1 + l_\mathbf{Q}^{p_\mathbf{Q}}\delta_\mathbf{Q}(\mathbf{m})/L^{p_\mathbf{Q}}\big]\big),$$
(4)

for $|\mathbf{q}| \ll \pi/2$. Any such ansatz that incorporates subleading finite-size effects must satisfy three conditions: First, the data for various sizes, when plotted against the scaling argument suggested by such an ansatz, must appear to collapse onto a single curve that defines the corresponding scaling function g. Second, the L dependence of S^z at each value of $\mathbf{m}$ should fit well to the form $A_\mathbf{m} + B_\mathbf{m}/L^p$ in which p is fixed by the choice made for the scaling variable earlier. Third, $A_\mathbf{m}$ and $B_\mathbf{m}$ must be consistent with expectations derived from the choice of scaling variable. More explicitly, $A_\mathbf{m} = g(\mathbf{m})$, and $B_\mathbf{m} = l\delta(\mathbf{m})\mathbf{m} \cdot \nabla_m g$. These three conditions hold at both peaks, and the subscripts indicating the peak in question can be temporarily omitted from g, δ, l, and p.

Before we use this framework to analyze our data, two points need to be made. The first is that the range of sizes available is not large enough to allow a unique determination of the best-fit values for $A_\mathbf{m}$, $B_\mathbf{m}$, and p from fits to the L dependence at each $\mathbf{m}$. This is because the deviations from perfect scaling are rather small, and as a result, one needs a very large range in L to pin down the best-fit p. With our limited range in L, a range of p gives equivalently good fits for the L dependence at each $\mathbf{m}$. Each choice of p in this

range fixes a best-fit value of $A_\mathbf{m}$ and $B_\mathbf{m}$ when one fits the L dependence at individual $\mathbf{m}$.

Likewise, the deviations from perfect scaling are too small to uniquely fix p, δ, and l by demanding the best scaling collapse for all the data plotted against the scaling variable corresponding to these choices for p, δ, and l. One obtains scaling collapse that looks equally good to the eye for a range of p, and for at least two simple choices for the function δ: $\delta(\mathbf{m}) = 1$ and $\delta(\mathbf{m}) = |\mathbf{m}|$. The best one can do is to fix l uniquely after choosing a p within this range and making one of these two choices for δ.

In view of this uncertainty, the self-consistency conditions outlined above (which relate the best-fit $A_\mathbf{m}$ and $B_\mathbf{m}$ to the choices made for δ and l which define the corresponding scaling variable, and to the function g defined by the resulting scaling collapse) are particularly useful in fixing the form of the finite-size corrections from the available data. We have therefore systematically scanned over the range of p that yields a viable description for both simple choices of the function δ. For each choice of δ and p, we have determined the value of l that yields the best scaling collapse, as well as obtained the best-fit $A_\mathbf{m}$ and $B_\mathbf{m}$ from fits to the L dependence at each individual $\mathbf{m}$. We have then tested for self-consistency as outlined above.

Based on this extensive study, we conclude that finite-size corrections to perfect scaling take on the form corresponding to $\delta_0(\mathbf{m}) = \delta_\mathbf{Q}(\mathbf{m}) = |\mathbf{m}|$, $l_0 = 3.8(1)$, $l_\mathbf{Q} = 6.5(1)$, $p_0 = 1.0(2)$, and $p_\mathbf{Q} = 1.2(1)$. Furthermore, the scaling functions $g_0(x)$ and $g_\mathbf{Q}(x)$ both take on power-law forms for not too small x, consistent with the expectations from the scaling theory for impurity response[18] which fixes the power-law forms of both functions in terms of a single impurity exponent η': $g_0(\mathbf{m}) \sim |\mathbf{m}|^{-\eta'/2}$ and $g_\mathbf{Q}(\mathbf{m}) \sim |\mathbf{m}|^{-(3-\eta+\eta')/2}$.

This scaling collapse is shown in Fig. 2, while the corresponding fits to the data at fixed $\mathbf{m}$, from which the values of $A_\mathbf{m}$ and $B_\mathbf{m}$ are obtained, are shown in Fig. 3. The $A_\mathbf{m}$ thus obtained are marked in Fig. 2 and seen to fall right on top of the composite curves produced by the data collapse which define the corresponding scaling function g_0 and $g_\mathbf{Q}$. These scaling functions are fit to power-law forms expected from the scaling theory for the impurity spin texture, and both scaling functions are seen to be well-described by power laws determined by a *single* impurity exponent $\eta' = 1.0(1)$,
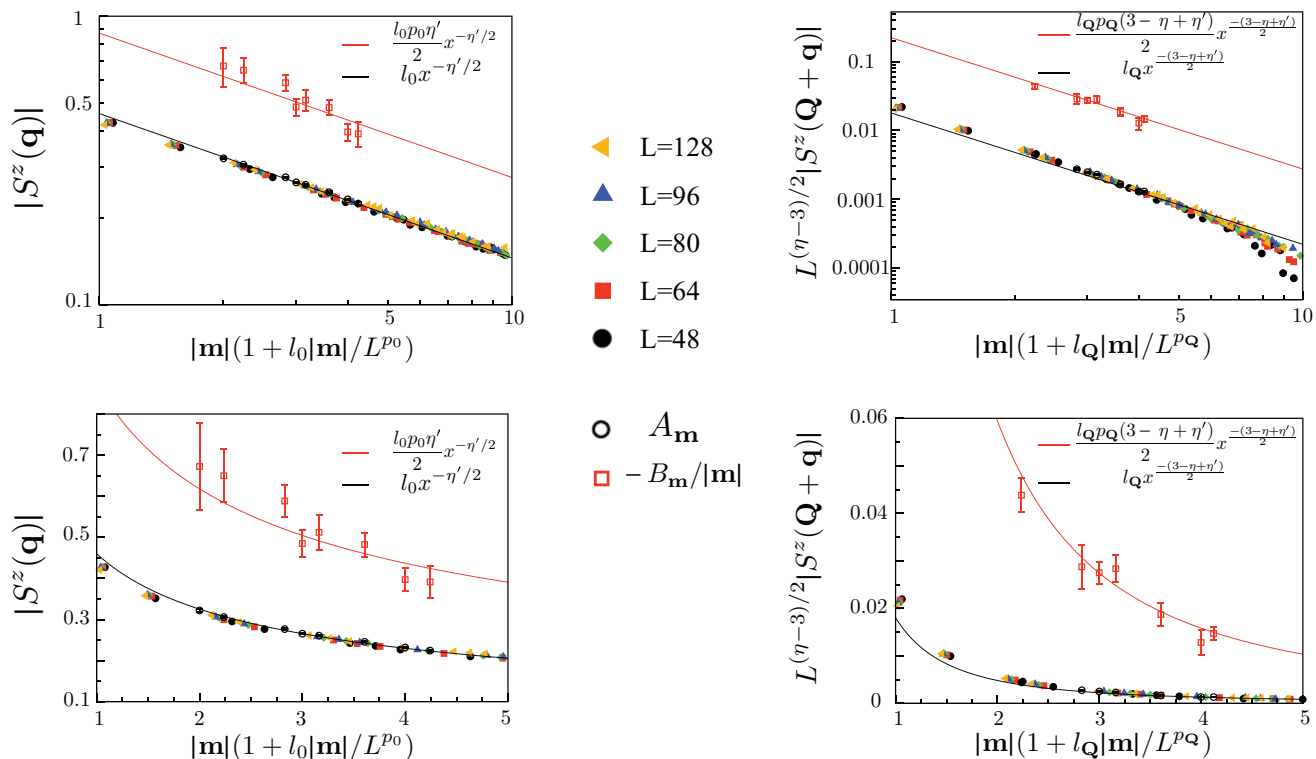
FIG. 2. (Color online) Scaling collapse of $|S^z(\mathbf{k})|$ as a function of $\mathbf{m} = \mathbf{q}L/2\pi$ at the Néel-VBS transition in the SU(3) symmetric J-Q model for various L in accordance with the ansatz Eq. (4) for $\mathbf{k} = \mathbf{Q} + \mathbf{q}$ (right panels) and $\mathbf{k} = \mathbf{q}$ (left panels). Also shown are points representing $A_{\mathbf{m}}$, which fall right on top of the scaling functions g_0 and $g_{\mathbf{Q}}$ defined by the scaling collapse. We also display the $|\mathbf{m}|$ dependence of $B_{\mathbf{m}}$ and compare it against the expected dependence required by self-consistency. Data in the vicinity of both peaks are shown in linear scale (bottom panels) as well as logarithmic scale (top panels). Straight lines on the log-log plots display the power-law nature of the scaling functions, with both scaling functions controlled by the single impurity scaling exponent η' as indicated in the text. The linear scale of the bottom panels highlights the quality of collapse.

as expected from the scaling analysis. Also shown in Fig. 2 is the comparison between the best-fit $B_{\mathbf{m}}$ obtained from the fits in Fig. 3 and their expected $|\mathbf{m}|$ dependence obtained from the self-consistency. Again, we see that the $|\mathbf{m}|$ dependence of $B_{\mathbf{m}}$ is consistent with that expected from the consistency condition.

Thus, conventional finite-size corrections to scaling appear to give a completely consistent account of our data for both peaks in the Fourier transform of the impurity spin texture. In this context, it is interesting to note that multiplicative

corrections (which amount to violations of scaling) appear to be favored over such conventional additive corrections to scaling by the author of Ref. 17 when describing the behavior of the spin stiffness at the transition in the pure system.

V. DISCUSSION

The fact that the L dependence of the impurity-induced spin texture of the SU(3) model studied there can be described well in terms of ordinary finite-size corrections to scaling should
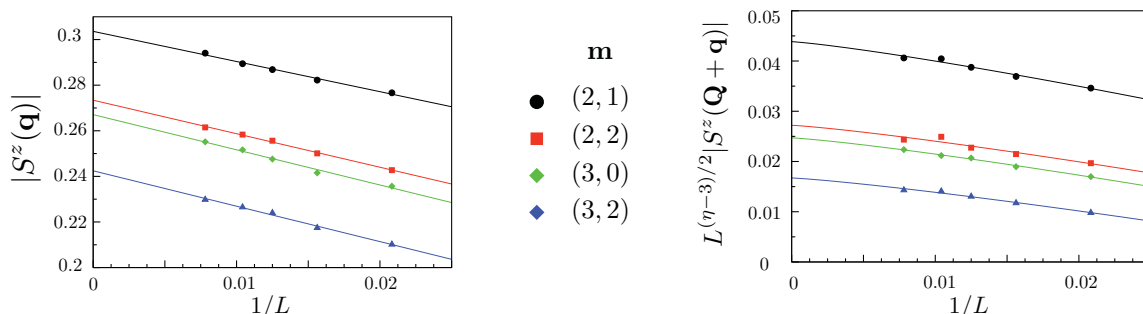

FIG. 3. (Color online) L dependence of $|S^z(2\pi\mathbf{m}/L)|$ (left panel) and of $|S^z(\mathbf{Q} + 2\pi\mathbf{m}/L)|$ (right panel) at the Néel-VBS transition in the SU(3) symmetric J-Q model at various $\mathbf{m}$. Solid lines denote fits to the form mentioned in text, and the legends indicate $\mathbf{m} = (m_x, m_y)$ corresponding to each curve.

be contrasted with the findings of our recent study[14] of the spin texture in the SU(2) symmetric $S = 1/2$ J-Q models on the square lattice. There, we found that any attempt to fit the deviations from scaling to this conventional form resulted in unphysically large l and very small p in the SU(2) case. As a result, one was forced in the SU(2) case to consider either an unconventional form of scaling argument proportional to $\mathbf{m}/L^p$ with very small p, or admit the possibility of logarithmic violations of scaling, as reflected in an argument of the form $\mathbf{m}/\log(L/l)$ for the scaling function. These two possibilities are in fact numerically indistinguishable from each other in the SU(2) case over the range of available sizes. Since the former has no known basis while the latter is a known to be a possible consequence of marginally irrelevant operators in the renormalization group description of phase transitions, the most natural conclusion consistent with the numerical evidence was that there are logarithmic violations of scaling due to the presence of a marginal operator in the SU(2)

case.[13,14] That this is not the case at the SU(3) critical point is the central message of our work.

Our results thus support the scenario that some operator that is irrelevant at fixed points describing Néel-VBS transitions for $N \geqslant 3$ becomes marginal at or near $N = 2$. We hope these results will motivate further study of the field-theoretical description of the critical theories underlying these interesting, but still only partially understood, quantum phase transitions.

[1] H. Alloul, J. Bobroff, M. Gabay, and P. J. Hirschfeld, Rev. Mod. Phys. **81**, 45 (2009).

[2] N. Read and S. Sachdev, Phys. Rev. B **42**, 4568 (1990).

[3] N. Read and S. Sachdev, Nucl. Phys. B **316**, 609 (1989).

[4] T. Senthil, A. Vishwanath, L. Balents, S. Sachdev, and M. P. A. Fisher, Science **303**, 1490 (2004); T. Senthil, L. Balents, S. Sachdev, A. Vishwanath, and M. P. A. Fisher, Phys. Rev. B **70**, 144407 (2004).

[5] Only quadrupled hedgehog defects and their bound states can be important at long length scales, because other hedgehog defects carry an oscillating Berry phase which renders them irrelevant to long-distance physics.

[6] A. B. Kuklov, M. Matsumoto, N. V. Prokof'ev, B. V. Svistunov, and M. Troyer, Phys. Rev. Lett. **101**, 050405 (2008).

[7] O. I. Motrunich and A. Vishwanath, e-print arXiv:0805.1494.

[8] A. Kuklov, M. Matsumoto, N. Prokof'ev, B. Svistunov, and M. Troyer, e-print arXiv:0805.2578.

[9] A. W. Sandvik, Phys. Rev. Lett. **98**, 227202 (2007).

[10] R. G. Melko and R. K. Kaul, Phys. Rev. Lett. **100**, 017203 (2008).

[11] F. J. Jiang, M. Nyfeler, S. Chandrasekharan, and U. J. Wiese, J. Stat. Mech.: Theory Exp. (2008) P02009.

[12] J. Lou, A. W. Sandvik, and N. Kawashima, Phys. Rev. B **80**, 180414 (2009).

[13] A. W. Sandvik, Phys. Rev. Lett. **104**, 177201 (2010).

[14] A. Banerjee, K. Damle, and F. Alet, Phys. Rev. B **82**, 155139 (2010).

[15] K. Harada, N. Kawashima, and M. Troyer, Phys. Rev. Lett. **90**, 117203 (2003).

[16] K. S. D. Beach, F. Alet, M. Mambrini, and S. Capponi, Phys. Rev. B **80**, 184401 (2009).

[17] R. K. Kaul, e-print arXiv:1010.1937.

[18] K. H. Hoglund, A. W. Sandvik, and S. Sachdev, Phys. Rev. Lett. **98**, 087203 (2007).

[19] M. A. Metlitski and S. Sachdev, Phys. Rev. B **76**, 064423 (2007).

[20] E. H. Lieb and D. C. Mattis, J. Math. Phys. **3**, 749 (1962).

[21] J. B. Parkinson, J. Phys. C **10**, 1735 (1977).

[22] A. Banerjee and K. Damle, J. Stat. Mech. (2010) P08017.

[23] A. W. Sandvik and H.-G. Evertz, Phys. Rev. B **82**, 024407 (2010).

[24] This value of η lies slightly outside the error bars of the higher value quoted in Ref. 12. This is possibly due to the different estimate of the critical point $J/Q|_c$, since we find that the original estimate of the critical point in Ref. 12 yields a higher value consistent with the original estimate of η.

[25] A. F. Albuquerque, F. Alet, P. Corboz, P. Dayal, A. Feiguin, S. Fuchs, L. Gamper, E. Gull, S. Guertler, A. Honecker, R. Igarashi, M. Koerner, A. Kozhevnikov, A. Laeuchli, S. R. Manmana, M. Matsumoto, I. P. McCulloch, F. Michel, R. M. Noack, G. Pawlowski, L. Pollet, T. Pruschke, U. Schollwock, S. Todo, S. Trebst, M. Troyer, P. Werner, and S. Wessel, J. Magn. Magn. Mater. **310**, 1187 (2007); M. Troyer, B. Ammon, and E. Heeb, Lect. Notes Comput. Sci. **1505**, 191 (1998); see [http://alps.comp-phys.org].